DOI: 10.1002/ejic.200900122

Crystal Structures and Solution Behavior of Paramagnetic, Trinuclear, Mixed-Valent Cobalt Complexes with Salen-Type Ligands

Lassaad Mechi,[a] Patrizia Siega,[a] Renata Dreos,*[a] Ennio Zangrando,[a] and Lucio Randaccio*[a]

Keywords: Mixed-valent compounds / Cobalt / N,O ligands / Solid-state structures / NMR spectroscopy

New trinuclear mixed-valent Co^{III}-Co^{II}-Co^{III} complexes with salen-type ligands have been synthesized and characterized both in the solid state and in solution. These complexes comprise a central $CoCl_2$ unit connecting two [RCo(4,4′,7,7′tmsalen)] fragments with chlorides acting as bridging ligands between the metals, while the central Co^{II} ion completes its octahedral coordination through the salen oxygen donors. Complex **1** (R = CH_2Cl), which has *cis* Cl ligands at the central Co^{II} ion, has approximate C_2 symmetry, whereas the centrosymmetric complex **2** (R = CF_3CH_2) contains *trans* Cl ligands (C_{2h} symmetry). Complexes **1** and **2** are paramagnetic with magnetic moments of 4.7 and 4.4 μ_B, respectively, which indicate the presence of a high-spin Co^{II} center in the molecule. The ^1H NMR spectra, which spread over a range of nearly 190 ppm, are consistent with the presence of both *cis* and *trans* isomers in solution (with *cis* being the prevailing species), and indicate that exchange is slow on the NMR time-scale. Isotropically shifted ^1H NMR signals have been fully assigned by comparison with those of appropriately substituted complexes and by T_1 measurements and 2D exchange experiments (EXSY). The K constant for the *trans* ⇄ *cis* equilibrium, as evaluated from the ^1H NMR signal intensity ratio at various temperatures, has allowed us to estimate, at least qualitatively, the thermodynamic parameters $\Delta H°$ and $\Delta S°$.

Introduction

Cobalt complexes with salen-type ligands [salen = *N*,*N*′-ethylenebis(salicylideneiminato); Scheme 1] have a wide range of applications. In particular, organometallic Co^{III}(salen) complexes have been studied as vitamin B_{12} models[1] and Co^{II}(salen), which is classified as an oxygen carrier,[2] has been used as a catalyst for the oxidation of organic substrates.[3] Some years ago, we reported the synthesis and characterization of several organometallic [RCo(4,4′,7,7′tmsalen)] derivatives (4,4′,7,7′tmsalen = 4,4′,7,7′-tetramethylsalen; Scheme 1).[4,5] An X-ray structural determination showed that these [RCo(4,4′,7,7′tmsalen)] complexes adopt a planar *trans* geometry (also in the dimeric form), except for the case where R is CH_2Cl. In that case, the reaction gave rise, beside the expected *trans* organometallic species, to the *cis*-β organometallic derivative $[Co(4,4′,7,7′tmsalenCH_2)(py)(H_2O)]^+$ upon intramolecular reaction of the axial chloromethyl group with the equatorial chelate.[5,6]

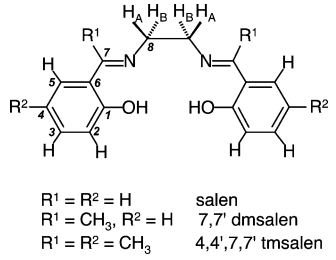

Scheme 1.

The ability of Co(salen) complexes to act as bidentate chelating ligands for both transition and non-transition metals to form dinuclear complexes has been known for a long time.[7] In spite of the increasing attention devoted to multinuclear transition metal complexes due to their potential use as catalysts[8] or to model active sites of metalloproteins,[9] linear trinuclear mixed-valent cobalt complexes with salen-type ligands are rare,[10] and most of them have been serendipitously obtained. Furthermore, a detailed characterization of these species in solution by ^1H NMR spectroscopy has never been performed. Indeed, the presence of the paramagnetic Co^{II} ion complicates the assignment of the signals despite the fact that Co^{II} complexes with organic ligands generally afford reasonably well-resolved ^1H NMR spectra.[11]

We have found that the [RCo(4,4′,7,7′tmsalen)] complexes and the strictly related [RCo(7,7′dmsalen)] deriva-

[a] Dipartimento di Scienze Chimiche, Università di Trieste, Via Licio Giorgieri 1, 34127, Trieste, Italy
Fax: +39-040-5583903
E-mail: dreos@units.it
lrandaccio@units.it

Supporting information for this article is available on the WWW under http://www.eurjic.org or from the author.

tives (7,7′dmsalen = 7,7′-dimethylsalen; Scheme 1) allow the formation of trinuclear mixed-valent complexes of different configuration in the presence of a stoichiometric amount of $CoCl_2$. Herein we report the synthesis, X-ray single crystal structure, and the full assignment of the isotropically shifted ^1H NMR spectra of [{(ClCH$_2$)Co(4,4′7,7′tmsalen)}$_2$CoCl$_2$] (**1**), [{(CF$_3$CH$_2$)Co(4,4′7,7′tmsalen)}$_2$CoCl$_2$] (**2**), and [{(ClCH$_2$)Co(7,7′dmsalen)}$_2$CoCl$_2$] (**3**). An estimate of $\Delta H°$ and $\Delta S°$ for the conformational equilibrium of complexes **1** and **2** in solution is also reported.

Results and Discussion

The trinuclear complexes **1** and **2** were obtained by mixing the appropriate [RCo(4,4′,7,7′tmsalen)]$_2$ complex[4] with a stoichiometric amount of $CoCl_2$ in CH_2Cl_2/*i*PrOH. The metallacyclization of [(ClCH$_2$)Co(4,4′,7,7′tmsalen)]$_2$[5,6] under these experimental conditions is slow enough to allow the isolation of **1**. Complex **3** was synthesized in a similar manner with the aim of facilitating the assignment of the ^1H NMR spectra.

The reaction between [(ClCH$_2$)Co(4,4′,7,7′tmsalen)]$_2$ and $CoCl_2$ was followed by ^1H NMR spectroscopy (Figure 1). Thus, a solution of $CoCl_2$ in *i*PrOH was added to a solution of [(ClCH$_2$)Co(4,4′,7,7′tmsalen)]$_2$ in $CDCl_3$ in a 0.25:1 molar ratio. The spectrum recorded immediately after the addition shows the presence of the trinuclear complex, while the signals in the range δ = 0–10 ppm, arising from the residual mononuclear [(ClCH$_2$)Co(4,4′,7,7′tmsalen)][12] become broader and are spread out. A second spectrum recorded after 10 minutes is entirely superimposable on the former, thus showing that trinuclear complex formation is relatively fast. The spectra recorded after further additions of $CoCl_2$ (molar ratio 0.50:1 and 0.75:1) show an increase of the intensity of the signals of **1**, while the peaks in the diamagnetic range become very broad. The spectrum recorded after the addition of a stoichiometric amount of $CoCl_2$ (1:1) shows the disappearance of the latter peaks, thus indicating that the formation of **1** is practically complete.

A spectrophotometric titration of [(ClCH$_2$)Co(4,4′,7,7′tmsalen)]$_2$ with $CoCl_2$ shows a clean isosbestic point at 320 nm for [$CoCl_2$]/[(ClCH$_2$)Co(4,4′,7,7′tmsalen)]$_2$ ratios ≤ 1 (Figure S1, Supporting Information). New species {most likely, the dinuclear complex [{(ClCH$_2$)Co(4,4′,7,7′tmsalen)}$CoCl_2$], with $CoCl_2$ coordinated by the phenoxo oxygen atoms of 4,4′,7,7′tmsalen} appear at higher [$CoCl_2$]/[(ClCH$_2$)Co(4,4′,7,7′tmsalen)]$_2$ ratios (up to 8).

Crystal Structure of Complexes 1 and 3

The ORTEP drawing of one of the two independent molecules found in **1** is depicted in Figure 2. The trinuclear complex can be described as containing a central $CoCl_2$ unit connecting two [(ClCH$_2$)Co(4,4′,7,7′tmsalen)] fragments, with the chlorides acting as bridging ligands between the terminal Co(4,4′,7,7′tmsalen) units and salen oxygen donors completing the octahedral coordination environment of the central metal ion. This complex, which has *cis* Cl ligands at the central Co^{II} ion, has approximate C_2 symmetry. This stereochemistry generates an element of chirality in the complex, with possible Λ and Δ configurations. Both these enantiomers are present in the unit cell (noncentric space group *Pna*2$_1$) as crystallographically independent molecules. The molecules A (Figure 2) and B (Figure S2) differ due to slight modifications in their conformation, with the main variation being the orientation assumed by the axial CH_2Cl groups. The octahedral geometry about the cobalt ions in the two independent molecules is severely distorted from ideal values; a selection of bond lengths is given in Table 1. The 4,4′,7,7′tmsalen ligand coordinates Co(1) and Co(3) in the four equatorial positions, with a CH_2Cl and a bridging chloride located at the axial sites. The Co–N and Co–O bond lengths are comparable within 2–3σ [range: 1.844(8)–1.902(7) Å], and the axial Co–C and Co–Cl bond lengths fall in the range 1.939(9)–2.077(13) and 2.507(3)–2.625(3) Å, respectively. The Co(2)–O distances in

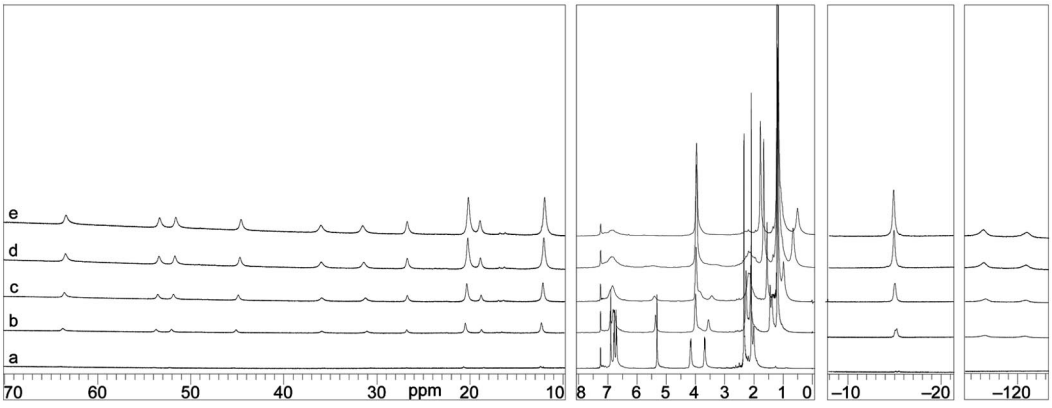

Figure 1. Formation of **1**, as followed by ^1H NMR spectroscopy. Spectrum of a solution of [(ClCH$_2$)Co(4,4′,7,7′tmsalen)]$_2$ in $CDCl_3$ (14 mg in 0.6 mL) (a). Spectra after the stepwise addition of $CoCl_2$ in 2-propanol [$CoCl_2$]/[(ClCH$_2$)Co(4,4′,7,7′tmsalen)]$_2$ ratio: 0.25 (b), 0.50 (c), 0.75 (d), and 1 (e).

the $Co(2)O_4Cl_2$ chromophore core vary from 2.081(5) to 2.202(6) Å, and the Co^{II}–Cl bond lengths are around 0.15–0.20 Å shorter than the Co^{III}–Cl ones due to the strong *trans* influence exerted by the axial R group on the latter metal ions. The metals are separated by 2.843(2) and 2.839(2) Å in molecule A and by 2.854(2) and 2.850(2) Å in the other, with an average Co–Co–Co angle of 163.60(6)°. The Co–Cl–Co bridging angles fall in the range 68.43(7)–70.70(7)°.

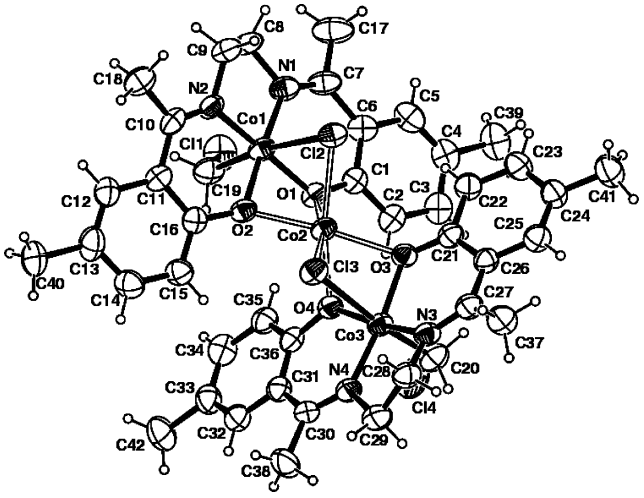

Figure 2. ORTEP drawing (35% ellipsoid probability) of molecule A (Λ enantiomer) in compound **1**. The same scheme also applies to molecule B and to complex **3**, where methyl groups C39–C42 are substituted with H atoms.

Table 1. Selected bond lengths [Å] for **1** and **3**.

	1, Molecule A	**1**, Molecule B	**3**
Co(1)–O(1)	1.876(5)	1.878(5)	1.866(4)
Co(1)–O(2)	1.892(6)	1.872(6)	1.887(5)
Co(1)–N(1)	1.844(8)	1.880(7)	1.861(6)
Co(1)–N(2)	1.902(7)	1.895(6)	1.864(5)
Co(1)–C(19)	1.951(10)	1.948(9)	2.074(10)
Co(1)–Cl(2)	2.532(3)	2.507(3)	2.600(2)
Co(2)–O(1)	2.194(6)	2.202(6)	2.104(4)
Co(2)–O(2)	2.080(6)	2.083(6)	2.097(4)
Co(2)–O(3)	2.136(6)	2.088(6)	2.113(4)
Co(2)–O(4)	2.081(5)	2.100(6)	2.112(4)
Co(2)–Cl(2)	2.408(2)	2.425(3)	2.407(2)
Co(2)–Cl(3)	2.414(3)	2.409(3)	2.402(2)
Co(3)–O(3)	1.864(5)	1.896(6)	1.879(4)
Co(3)–O(4)	1.871(6)	1.889(6)	1.879(4)
Co(3)–N(3)	1.891(8)	1.844(8)	1.884(5)
Co(3)–N(4)	1.879(7)	1.868(8)	1.881(5)
Co(3)–C(20)	1.939(9)	2.077(13)	1.952(7)
Co(3)–Cl(3)	2.625(3)	2.604(3)	2.516(2)
Co(1)–Co(2)	2.843(2)	2.854(3)	2.835(1)
Co(2)–Co(3)	2.839(2)	2.850(3)	2.836(1)

The 4,4′,7,7′tmsalen bound to Co(1) shows a sigmoidal conformation, while that at Co(3) is slightly bent (Figure 3); similar deformations are observed in the other enantiomer. The dihedral angles formed by the N_2O_2 donor plane and the two salicylaldiminate residues in the two molecules[13] are small [mean values at Co(1): 10.5° and 22.8°; mean values at Co(3): 16.7° and 2.0°; see Table 2]. The *cis* configuration exhibited by complex **1** forces the 4,4′,7,7′tmsalen ligands to be almost perpendicular to each other and the dihedral angles formed by the N_2O_2 planes to be 81.4(2)° and 83.6(2)° in molecules A and B, respectively.

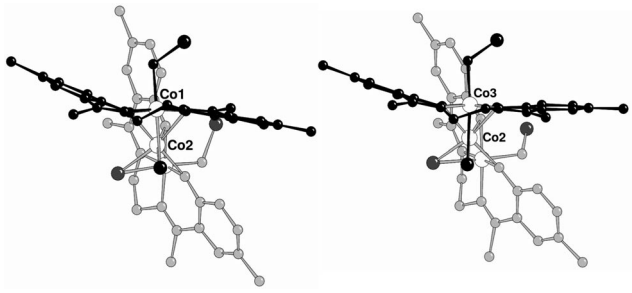

Figure 3. Side views of molecule A of **1** showing the 4,4′,7,7′tmsalen distortions from planarity at Co(1) and Co(3).

Table 2. Geometrical parameters defining the deformation in the salen moieties.

	1, Molecule A		**1**, Molecule B		**3**	
	Co1	Co3	Co1	Co3	Co1	Co3
$\alpha 1$ [°][a]	10.0(4)	16.6(2)	11.1(4)	16.8(2)	1.5(2)	12.0(2)
$\alpha 2$ [°]	22.9(3)	2.6(3)	22.7(3)	1.4(3)	17.4(2)	7.3(2)
β [°][b]	13.9(3)	17.3(2)	13.30 (3)	17.6(2)	16.1(2)	19.0(2)
γ [°][c]	81.4(2)		83.6(2)		81.8(1)	
d [Å][d]	0.089(4)	0.111(4)	0.051(4)	0.110(4)	0.096(3)	0.067(3)

[a] $\alpha 1$ and $\alpha 2$: dihedral angles between the mean Co coordination plane and salicylaldiminate residues. [b] β: dihedral angle between the salicylaldiminate half moieties. [c] γ: dihedral angle between the mean N1/O1/N2/O2 and N3/O3/N4/O4 planes. [d] d: displacement of the metal from the N_2O_2 equatorial plane towards the alkyl ligand.

The X-ray structural determination of **3** reveals that the complex also crystallizes with a *cis* configuration. The overall geometry is similar to that of complex **1**, and its ORTEP picture is provided in Figure S3 (Supporting Information). The Co(1)–Co(2) and Co(2)–Co(3) distances are 2.835(1) and 2.836(1) Å, respectively, with an intermetallic angle of 163.51(4)°. The coordination geometry and salen deformations (Tables 1 and 2) are very similar to those found in **1** and will not be discussed further.

Crystal Structure of Complex 2

Figure 4 displays an ORTEP drawing of the trinuclear complex; a selection of coordination bond lengths are given in Table 3. Two [(CF_3CH_2)Co(4,4′,7,7′tmsalen)] fragments are connected by a $Co^{II}Cl_2$ unit in a centrosymmetric arrangement such that Co^{II} is bound to two salen chelating units in the equatorial positions and chloride in the axial ones. The distortions observed in the octahedral coordination geometry of the cobalt ions resemble those found in **1** and **3**. The 4,4′,7,7′tmsalen ligand coordinates Co(1) at the four equatorial positions with comparable Co–N and Co–O bond lengths [range: 1.875(4)–1.886(4) Å], while a CF_3CH_2 and a bridging chloride complete the octahedral geometry [Co(1)–C = 1.965(7) Å; Co(1)–Cl = 2.561(2) Å]. The central CoO_4Cl_2 chromophore shows Co(2)–O and

Co(2)–Cl distances of 2.092(4) (mean value) and 2.441(2) Å, respectively. The collinear metals are separated by 2.832(1) Å and the bridging angle at Cl(1) is 68.91(5)°.

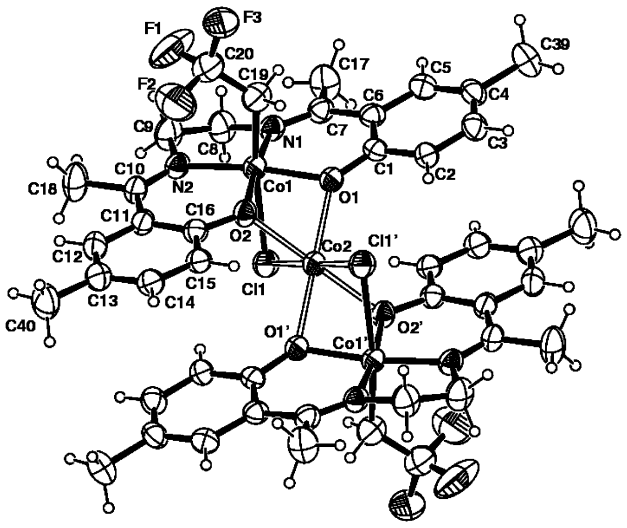

Figure 4. ORTEP drawing (35% ellipsoid probability) of complex **2** located on an inversion center.

Table 3. Selected bond lengths [Å] for **2**.

Co(1)–O(1)	1.875(4)	Co(1)–Cl(1)	2.561(2)
Co(1)–O(2)	1.881(3)	Co(2)–O(1)	2.094(4)
Co(1)–N(1)	1.886(4)	Co(2)–O(2)	2.091(4)
Co(1)–N(2)	1.879(5)	Co(2)–Cl(1)	2.441(2)
Co(1)–C(19)	1.965(7)	Co(1)–Co(2)	2.832(1)

The equatorial 4,4′,7,7′tmsalen ligand has an almost flattened conformation, as indicated by the dihedral angles between the N_2O_2 donor plane and the two salicylaldiminate residues of 11.8(2)° and 3.5(2)°,[13] while the angle, β, between the salicylaldiminate moieties is 8.7(2)°. The almost coplanar arrangement of the salen ligand in **2** may be due to the presence of the bulkier CF_3CH_2 axial ligand.

We can conclude from the above data that the different configurations observed in these complexes (*cis* in complexes **1** and **3** vs. *trans* in **2**) do not affect the coordination bond lengths and angles or the Co–Co distances, which are comparable within their e.s.d.'s. The Co–Co–Co angle inside the complex core of **1** and **3** (ca. 163.5°) shows small deviations from the linear arrangement of 180° observed in **2** and imposed by the crystallographic symmetry. The small deformations observed in the salen ligands are likely due to packing forces.

Although both isomers are present in solution (see below), the *cis* or *trans* configuration detected in the solid state for these complexes seems to be governed by the steric properties of the axial ligand. The structural characterization of similar trinuclear cobalt complexes shows either a *cis* or *trans* configuration, with the metals bridged by acetato anions in all the examples retrieved except for one complex with a sulfite[10a] and, more recently, one with a pseudohalide[10g] bridge, which formally replace the chloride of the present complexes. It is worthwhile noting that the intermetallic distances in either $Co^{II}{}_3$[14] or mixed-valent $Co^{III}Co^{II}Co^{III}$ trinuclear species[10] are significantly longer (>3.0 Å) than those of around 2.8 Å reported here. From a structural point of view, all the species isolated with a *trans* configuration appear to have bulky ligands [i.e., dmf, propanol, pyridine, CH_2CF_3 (**2**)] that complete the octahedral geometry of the outer cobalt ions. In such a configuration, these axial ligands avoid steric clashes with the phenyl ring of the other terminal Co(salen-type) fragment, and our hypothesis regarding ligand bulkiness is corroborated by the observation that the ethylene bridge in the present complexes is more flattened in **2** [N–C–C–N torsion angle of 27.3(9)°] when compared with the values observed in **1** and **3** [absolute value range 36.7(10)–46.6(12)°]. A *trans* arrangement is also observed with outer pentacoordinate cobalt ions,[14b–14d] where the Co(salen-type) fragment assumes a marked umbrella-shaped conformation (mean β = 55°). Complexes containing smaller axial ligands such as acetate or SCN (CH_2Cl in **1** and **3**) have been isolated in the solid state as their *cis* isomers,[10b,10d,10e] although other factors, such as solubility or solvation effects, might influence the configuration found in solid state.

Magnetic Measurements

The magnetic moments of **1** and **2** are 4.7 and 4.4 μ_B, respectively, which correspond to the presence of a high-spin Co^{II} in the molecule. Thus, the complexes contain low-spin Co^{III} ions and a high-spin Co^{II} i.e., they are Co^{III}(S = 0)–Co^{II}(S = 3/2)–Co^{III}(S = 0) trimers.

^{1}H NMR Spectroscopy

The ^{1}H NMR spectra of the trinuclear complexes in $CDCl_3$ show very similar features (Figure 5 and Figures S4 and S5 in the Supporting Information). For the sake of simplicity we will only describe the spectrum of **1** (Figure 5), which reveals the presence of both the *cis* and *trans* isomers in an approximately 4:1 ratio at 297.9 K. The spectrum shows 20 well-defined broad singlets spread over a range of nearly 190 ppm along with four additional peaks, which are hidden at room temperature but appear in the spectra at low temperature (Figure 6). If the intensity of the singlet resonating at δ = 51.9 ppm is fixed equal to one proton, the high-integrating set consists of 16 singlets, 12 of which integrate for one proton and four for three protons, in agreement with the C_2 symmetry found in the X-ray structure of **1**. The low-integrating set contains eight signals, five of which integrate for one proton, one for two protons, and two for three protons (signal at δ = 49.2 ppm set equal to one proton), in agreement with a C_{2h} symmetry, as found in the X-ray structural determination of complex **2**. It is noteworthy that the predominant isomer observed in solution for **2** is still **2**-C_2 (Figure S4) even though this complex

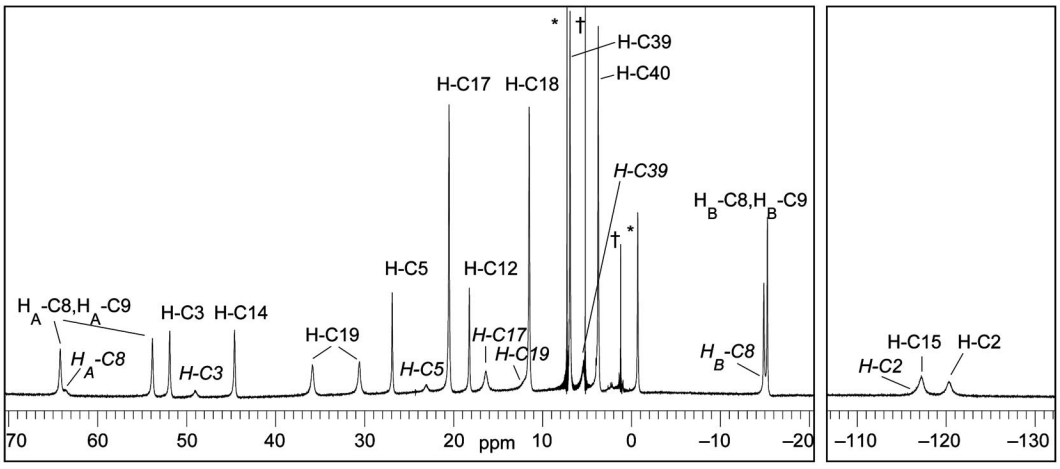

Figure 5. ^{1}H NMR spectrum of **1** in $CDCl_3$. Signals of $CDCl_3$ and H_2O are marked with an asterisk, and those of impurities with a dagger. Numbering of the signals of **1**-C_2 and **1**-C_{2h} (printed in *italics*) corresponds to that used in the crystal structures.

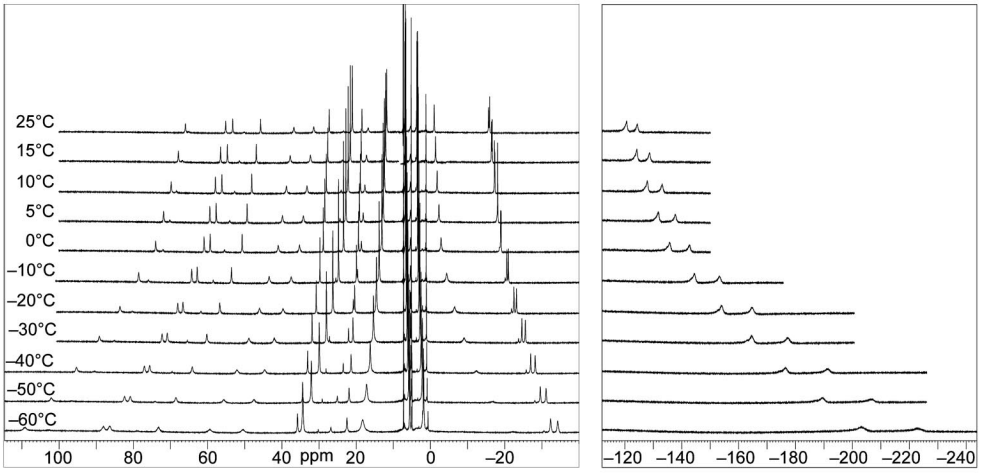

Figure 6. Variable-temperature ^{1}H NMR spectra of **1** in $CDCl_3$.

shows C_{2h} symmetry in the solid state. Small crystals of **2**-C_{2h} precipitated after some days from the solution used to record the ^{1}H NMR spectrum.

Below we describe first the assignment of the spectrum of **1**-C_2 (high-integrating set) and then that of **2**-C_{2h} (low-integrating set); the spectra of **1**-C_{2h} and **2**-C_2 were assigned by analogy.

Assignment of the ^{1}H NMR Spectrum of 1-C_2 by Substitution and T_1 Measurements

The resonances at δ = 3.7, 6.9, 11.5, and 20.5 ppm were assigned to the equatorial methyls (C39, C40, C41, C42) on the basis of their integrated intensity. The signals in the diamagnetic range were assigned to the methyls C39 and C40, which are more distant from the paramagnetic center.

The axial CH_2Cl group was assigned by comparing the spectra of **1** and [{(CH_3)Co(4,4′,7,7′tmsalen)}$_2$$CoCl_2$], which was synthesized in situ from [(CH_3)Co(4,4′,7,7′tmsalen)] and $CoCl_2$. The only significant difference is the presence of two peaks integrating for one proton at δ = 30.6 and 35.8 ppm in the former spectrum, while only one peak at δ = 31.5 ppm, integrating for three protons, is present in the latter (Figure S6). The two peaks were therefore assigned to the protons of the axial group, which are diastereotopic owing to the lack of symmetry of the two halves of the adjacent 4,4′,7,7′tmsalen moiety in **1**. This assignment was further confirmed by comparison with the spectrum of [{(CD_3)Co(4,4′,7,7′tmsalen)}$_2$$CoCl_2$], synthesized in situ from [(CD_3)Co(4,4′,7,7′tmsalen)] and $CoCl_2$, which contains no peaks in the range δ = 28–40 ppm (Figure S6).

The assignment of the remaining resonances is less obvious, although useful information can be obtained from an analysis of the longitudinal relaxation times (T_1). If the dipolar mechanism dominates the nuclear relaxation rates, as is usually the case for Co^{II} complexes, T_1 should vary linearly with the sixth power of the distance between the resonating nucleus and the paramagnetic center.[11,15] Thus, the distance between a proton and the Co^{II} ion can be estimated from Equation (1)

$$r_{Co-H} = r_{ref} (T_1/T_{1ref})^{1/6} \quad (1)$$

where r_{ref} is the distance between the Co^{II} center and the rigid reference proton with relaxation time T_{1ref}, and T_1 is the relaxation time of the proton under examination. The crucial step is the detection of a reliable reference proton, since the protons already assigned are not suitable for this purpose due to their rotational mobility. One of the 4,4′,7,7′ tmsalen ring protons would be the most appropriate choice, but this requires a previous independent assignment. For this purpose, complex **3**, where methyl groups C39–C42 of **1** (Figure 2) are replaced by H atoms, was synthesized and structurally characterized (Figure S3). The ^1H NMR spectrum of **3** is very similar to that of **1** but lacks the signals at δ = 3.7 and 6.9 ppm, thus confirming that these arise in **1** from the methyls C39 and C40 (now replaced by H atoms; Figure S5). The two new peaks in the spectrum of **3**, which integrate for one proton, resonate at δ = –17.7 and –19.7 ppm. The T_1 relaxation times of these signals were measured and the higher value (92 ms), corresponding to the resonance at δ = –17.7 ppm, was assigned to the H atom bound to C13 as this is more distant from the Co^{II} center (Table 4). The relaxation time of C13-H was used as T_{1ref} in Equation (1). The relaxation times of the aromatic and methylene protons of **3** were then measured and the $r_{Co–H}$ distances calculated from Equation (1) and compared with those taken from the X-ray structure. As slight deviations from ideal C_2 symmetry are observed in the solid state, the arithmetic average of the distances between the Co^{II} center and the symmetry-related H atoms was used for comparison. The good agreement found for the aromatic protons allows their assignment (Table 5), but some discrepancies are evident for the methylene protons. Assignment of the aromatic protons of **1** was carried out by analogy with those of **3** and confirmed by T_1 measurements with C12-H as reference (Table 5). The resonances at δ = –15.3, –14.9, 53.8, and 64.2 ppm in the spectrum of **1**-C_2 must therefore arise from the diastereotopic methylene protons H_A and H_B of C8 and C9. Their assignment is discussed below.

Table 4. Longitudinal relaxation time at 298 K in $CDCl_3$ and Co^{II}–H distances calculated from the NMR spectroscopic data and measured from the X-ray structures for **1**-C_2, **2**-C_{2h}, and **3**-C_2.

Chemical shift [ppm]	T_1 [ms]	$r_{Co^{II}–H}$ calcd. [Å]	$r_{Co^{II}–H}$ exp. [Å][a]	Assignments
1-C_2				
Aromatic				
51.9	19	5.5	5.35	C3-H
44.6	20	5.5	5.67	C14-H
26.9	46	6.3	6.10	C5-H
18.2	48	6.4	6.37[b]	C12-H
–117.0	1.6	3.6	3.64	C15-H
–120.2	1.5	3.6	3.48	C2-H
Methylene				
64.2	9	4.8	5.05	C8-H_A or C9-H_A
53.8	11	5.0	5.97	C8-H_A or C9-H_A
–14.9	40	6.2	5.95	C8-H_B or C9-H_B
–15.3	40	6.2	6.01	C8-H_B or C9-H_B
3-C_2				
Aromatic				
53.3	20	5.3	5.42	C3-H
45.5	21	5.3	5.58	C14-H
28.0	52	6.2	6.20	C5-H
18.0	52	6.2	6.33	C12-H
–19.7	88	6.7	6.56	C4-H
–17.7	92	6.8	6.76[b]	C13-H
–112.1	17	3.5	3.48	C15-H
–115.2	13	3.3	3.23	C2-H
Methylene				
66.2	9.5	4.6	5.03	C8-H_A or C9-H_A
54.7	12	4.8	5.93	C8-H_A or C9-H_A
–16.0	43	6.0	5.95	C8-H_B or C9-H_B
–16.7	43	6.0	5.99	C8-H_B or C9-H_B
2-C_{2h}				
Aromatic				
51.5	29	5.7	5.44	C3-H
22.8	45	6.2	6.17[b]	C5-H
Methylene				
66.9	17	5.2	5.53	C8-H_A

[a] Average value (see text). [b] Reference proton.

Assignment of the ^1H NMR Spectrum of 2-C_{2h} by 2D Experiments and T_1 Measurements

The low-integrating set of signals in the spectrum of **2** at room temperature consists of six broad singlets. Two additional resonances (δ = –15.5 and –119.8 ppm) are overlapped by signals of **2**-C_2, although they can be picked out in the spectra at low temperature. The starting point for assigning the ^1H NMR spectrum of **2**-C_{2h} was the assignment of the signals of **2**-C_2, which was carried out by analogy with that of **1**-C_2 (Table 5). The 2D exchange (EXSY) experiments (Figure S7, Supporting Information) show cross peaks between C3-H and C14-H of **2**-C_2 and one proton of **2**-C_{2h}. The C3-H and C14-H protons, which are symmetry-equivalent in the starting mononuclear unit [(CF_3CH_2)Co(4,4′,7,7′tmsalen)], turn out to be non-equivalent upon coordination to the central Co^{II} ion in the chiral **2**-C_2 isomer. In fact, C3-H and C14-H exchange their position on going from the Δ to the Λ enantiomer and, furthermore, the exchange process involves the C_{2h} isomer. This three-site exchange is depicted in Scheme 2. The signal of the low-integrating set that gives the same cross peak must arise from the corresponding C3-H proton of **2**-C_{2h}, which was consequently assigned. Further cross peaks (observed between C5-H and C12-H of **2**-C_2 and C5-H of **2**-C_{2h}, C17-H and C18-H of **2**-C_2 and C17-H of **2**-C_{2h}, and C39-H and C40-H of **2**-C_2 and C39-H of **2**-C_{2h}) allowed the assignment of these protons for the **2**-C_{2h} isomer (Table 5). The assignment of the latter two signals to methyl groups was confirmed by the integrated intensities.

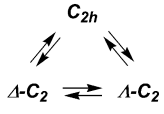

Scheme 2.

The data in Table 5 show that protons giving rise to cross peaks have close resonances, in agreement with the $r_{Co–H}$ distances from the X-ray structures. Consequently, the resonance at δ = –119.8 ppm (hidden at room temperature) was

Table 5. Assignment of ^{1}H NMR resonances of complexes **1**–**3**.[a]

Assignments		δ [ppm]					
		1-C_2	**1**-C_{2h}	**2**-C_2	**2**-C_{2h}	**3**-C_2	**3**-C_{2h}
C8-H_A or C9-H_A		64.2		65.5		66.2	
	C8-H_A		64.2		66.9		65.0
C8-H_A or C9-H_A		53.8		57.1		54.7	
C3-H		51.9		54.1		53.3	
	C3-H		49.2		51.5		50.0
C14-H		44.6		47.5		45.5	
C19-H		35.8		34.8		35.5	
C19-H		30.6		29.8		29.1	
C5-H		26.9		26.7		28.0	
	C5-H		23.1		23.0		24.1
C17-H		20.5		21.2		21.8	
C12-H		18.2		18.6		18.0	
	C17-H		16.3		17.3		17.3
C18-H		11.5		12.1		11.9	
	C19-H		11.5		9.9		11.9
C39-H		6.9		7.1			
	C39-H		5.4		5.4		
C40-H		3.7		4.2			
C8-H_B or C9-H_B		–14.9		–15.4		–16.0	
	C8-H_B		–14.9		–15.5		–16.7
C8-H_B or C9-H_B		–15.3		–15.5		–16.7	
C4-H						–17.7	
	C13-H						–19.7
C13-H						–19.7	
C15-H		–117.0		–119.8		–112.1	
	C2-H		–117.0		–119.8		–112.1
C2-H		–120.2		–125.9		–115.2	

[a] Atom numbering corresponds to that used in the crystal structure.

tentatively assigned to C2-H and those at δ = 66.9 and –15.5 ppm (hidden at room temperature) to the geminal diastereotopic protons of C8. To confirm this, T_1 measurements were carried out on the aromatic and methylene protons of **2**-C_{2h}. The $r_{Co–H}$ distances (calculated using C5-H as reference) were compared with those taken from the solid-state structure. A good agreement is observed for the aromatic C3-H proton (Table 4), thereby confirming its correct assignment, and for the proton resonating at δ = 66.9 ppm (H_A). This corresponds to the methylene proton above the equatorial plane pointing toward the μ-chloride and closer to the paramagnetic center than the geminal H_B. Hence, the resonance at δ = –15.5 ppm, whose relaxation time could not be measured because the signal is hidden at room temperature, was assigned to the latter. The dramatic difference in chemical shift between the geminal protons must be attributed to their different orientation (axial- vs. equatorial-like), thus suggesting a quite "frozen" conformation.[16] The remaining signal at δ = 9.9 ppm was assigned to the axial CF_3CH_2 protons, which are equivalent by symmetry in the *trans* isomer.

Assignment of the Methylene Protons of 1-C_2

Three of the $r_{Co–H}$ distances for methylene protons measured in the X-ray structures of **1** and **3** are relatively long (about 6 Å) and one is short (about 5 Å), whereas the values calculated from Equation (1) are two long (about 6 Å) and two short (less than 5 Å; Table 4). This suggests a different conformation of the ethylenediamine bridge in solution (probably more flattened) with respect to that in the solid state, which makes the assignment based on T_1 measurements difficult. A useful suggestion comes from the inspection of the low-integrating set in the spectrum of **1**, which corresponds to **1**-C_{2h} and has been assigned by analogy with the spectrum of **2**-C_{2h}. At –20 °C, the signals arising from the geminal methylene protons bound to C8 in **1**-C_{2h}, which are partially hidden at room temperature, resonate at δ = 80.3 and –21.8 ppm (Figure 6). The former is assigned to C8-H_A and the latter to C8-H_B by analogy with **2**-C_{2h} (see above). Correspondingly, the resonances at δ = 64.2 and 53.8 ppm for **1**-C_2 are assigned to H_A protons and those at δ = –14.9 and –15.3 ppm to H_B protons. Unfortunately, these results do not allow us to discriminate between the H_A (and H_B) protons bound to C8 and C9.

trans-cis Equilibrium in Solution

As pointed out above, the presence of two sets of signals in the ^{1}H NMR spectra of the trinuclear complexes indicates that both the *cis* and *trans* isomers are present in $CDCl_3$ solution. An alternative explanation could be formation of the dinuclear complex [{RCo(4,4′,7,7′tmsalen)}$CoCl_2$], with $CoCl_2$ coordinated by the phenoxo oxygen atoms of 4,4′,7,7′tmsalen. Although the symmetry of such a complex is consistent with the number of signals of the low-integrating set, the absence of resonances due to the mononuclear [RCo(4,4′,7,7′tmsalen)] fragment in the diamagnetic part of the spectrum, and the results of both the spectrophotometric and ^{1}H NMR ti-

trations (see above), allow us to rule out this hypothesis. The *cis* and *trans* isomers interconvert in solution, although the process is slow on the NMR time-scale because it requires the breaking of coordination bonds. Because of this slow exchange, the relative stabilities of the two isomers at various temperatures can be estimated by measuring the integrated signal intensities (*I*). For this purpose, the C3-H and C14-H signals of the *cis* and the C3-H signal of the *trans* isomer were chosen because they do not overlap when varying the temperature.

The *K* constant for the equilibrium *trans* ⇄ *cis* is

$K = [cis]/[trans] = 2I(cis)/I(trans)$

where *I*(*cis*) is the arithmetic average of the C3-H and C14-H intensities. The *K* values for **1** and **2** (Table 6) show that the equilibrium is slightly more shifted toward the *cis* isomer for **1** at room temperature.

Table 6. Equilibrium constants for the *trans* ⇄ *cis* equilibrium as a function of temperature.

T [°C]	*K*	
	Complex **1**	Complex **2**
–60.4	16.7	21.7
–50.2	15.4	18.6
–40.2	14.8	14.0
–30.2	11.8	12.4
–20.2	12.0	10.8
–10.2	10.3	9.8
–0.3	9.9	8.7
9.7	9.7	7.2
19.7	9.4	7.0
24.7	9.4	6.3
	$\Delta H°$ = –3.9 kJ mol^{-1}	$\Delta H°$ = –7.5 kJ mol^{-1}
	$\Delta S°$ = 5.7 J K^{-1} mol^{-1}	$\Delta S°$ = –9.9 J K^{-1} mol^{-1}

Variable-temperature ^{1}H NMR spectra for complexes **1** and **2** were recorded in the range from +25 to –60 °C (Figure 6). The total width of the spectrum increases markedly (from around 190 to around 330 ppm) upon decreasing the temperature. A plot of chemical shifts vs. $1/T$ is linear, according to the Curie law, as expected for a process based on pseudo-contact shifts (see Figure S8 in the Supporting Information).[11,15] Furthermore, the signal intensities vary with temperature, thus indicating that *K* is affected by temperature. In principle, plots of $\ln K_{eq}$ vs. $1/T$ allow the thermodynamic data for the equilibrium to be calculated (Figure S9, Supporting Information). Unfortunately, the intensity changes over the considered temperature range are small and the integration of signals is rather ambiguous due to the line broadness, which means that $\Delta H°$ and $\Delta S°$ can only be estimated (Table 6). However, the negative value of $\Delta S°$ for **2** could be related to a loss of rotational freedom of the bulky axial group on going from the *trans* to the *cis* isomer.

Conclusions

We have described new trinuclear mixed-valent Co^{III}-Co^{II}-Co^{III} complexes with salen-type ligands, which were prepared by mixing $[RCo(4,4',7,7'tmsalen)]_2$ and $CoCl_2$. The complexes were isolated as the *cis* (R = CH_2Cl, C_2 symmetry) or *trans* isomer (R = CF_3CH_2, C_{2h} symmetry), corresponding to the positions occupied by chloro ligands about the central Co^{II} ion, as confirmed by X-ray crystallography. Despite the presence of the paramagnetic metal center, the ^{1}H NMR spectra are reasonably well resolved and show that the *cis* and *trans* isomers interconvert slowly on the NMR time-scale in solution.

A full assignment of the isotropically shifted ^{1}H NMR signals for the two isomers has been carried out by comparison with those of appropriately substituted derivatives and by T_1 measurements and 2D exchange (EXSY) experiments. The *K* constant for the *trans* ⇄ *cis* equilibrium, as evaluated from the ^{1}H NMR signal intensity ratio at various temperatures, has allowed us to estimate, at least qualitatively, the thermodynamic data $\Delta H°$ and $\Delta S°$.

Experimental Section

General Information: NMR spectra were recorded with a Jeol EX-400 (^{1}H at 400 MHz, ^{13}C at 100.4 MHz) or a Jeol EX-270 (^{1}H at 270 MHz, ^{13}C at 67.8 MHz) spectrometer and were referenced to residual solvent protons. Electrospray mass spectra were recorded in positive mode with a Perkin–Elmer API 1 or Bruker ESQUIRE 4000 mass spectrometer. Magnetic susceptibility measurements were performed in $CDCl_3$ solution at room temperature by the Evans method with acetone as reference compound.[17] No diamagnetic corrections were applied. UV/Vis spectra were recorded with an Uvikon 941 spectrophotometer.

The complexes $[(ClCH_2)Co(4,4',7,7'tmsalen)]_2$, $[(CF_3CH_2)Co(4,4',7,7'tmsalen)]_2$, and $[(CH_3)Co(4,4',7,7'tmsalen)]_2$ were synthesized as described previously.[4,5] A slightly different synthesis for 7,7′dmsalen has been reported previously.[10a] All other reagents were analytical grade and were used without further purification.

Synthesis of $[\{(ClCH_2)Co(4,4',7,7'tmsalen)\}_2CoCl_2]$ (1): A solution of $[(ClCH_2)Co(4,4',7,7'tmsalen)]_2$ (0.100 g, 0.116 mmol) in CH_2Cl_2 (10 mL) was added to a solution of $CoCl_2{\cdot}6H_2O$ (0.028 g, 0.116 mmol) in 2-propanol (10 mL). The solution was filtered and set aside in the hood for crystallization. Partial evaporation of the solvent produced a dark solid, which was collected by filtration and kept over P_2O_5 overnight. X-ray quality crystals were obtained by slow evaporation of the reaction mixture. Yield 80 mg (70%). $C_{42}H_{48}Cl_4Co_3N_4O_4{\cdot}H_2O$ (1007.1): calcd. C 50.0, H 4.99, N 5.55; found C 49.2, H 4.81, N 5.09. UV/Vis (CH_2Cl_2): λ_{max} (ε) = 246 (9.17×10^4), 327 (1.90×10^4), 527 nm (1.74×10^3 M^{-1} cm^{-1}).

Synthesis of $[\{(CF_3CH_2)Co(4,4',7,7'tmsalen)\}_2CoCl_2]$ (2): This compound was synthesized by the same method described for **1**, starting from $[(CF_3CH_2)Co(4,4',7,7'tmsalen)]_2$ (0.100 g, 0.108 mmol) and $CoCl_2{\cdot}6H_2O$ (0.026 g, 0.109 mmol). Yield 51.4 mg (45%). $C_{44}H_{48}Cl_2Co_3F_6N_4O_4{\cdot}H_2O$ (1075.1): calcd. C 49.1, H 4.69, N 5.21; found C 49.6, H 5.07, N 4.95. UV/Vis (CH_2Cl_2): λ_{max} (ε) = 243 (7.77×10^4), 329 (1.69×10^4), 565 nm (1.28×10^3 M^{-1} cm^{-1}).

Synthesis of $[(CD_3)Co(4,4',7,7'tmsalen)]_2$: $[(CD_3)Co(4,4',7,7'tmsalen)]_2$ was synthesized following the procedure reported for $[(CH_3)Co(4,4',7,7'tmsalen)]_2$ starting from $[Co(4,4',7,7'tmsalen)(py)_2]ClO_4$ (0.5 g, 0.78 mmol) with CD_3I as alkylating agent.[4] Yield 250 mg (80%). $C_{42}H_{44}Co_2D_6N_4O_4$ (798.77): calcd. C 63.1, H 7.06, N 7.01; found C 62.9, H 6.30, N 6.92. ES-MS (CH_3OH): *m*/*z* (%) 799.5 (90) [M + H$^+$], 781 (100) [M – CD_3], 763.5 (62) [M – $2CD_3$], 400.0 (84) [M/], 381.5 (68) [M/2 – CD_3]. ^{1}H NMR ($CDCl_3$):

δ = 2.19 (s, 6 H, CH_3-Ph), 2.46 (s, 6 H, CH_3-C=N), 3.60 (m, 2 H, CH_2-CH_2), 4.05 (m, 2 H, CH_2-CH_2), 6.97 (d, ^3J = 8.0 Hz, 2 H, C2-H), 7.15 (m, 4 H, C3-H + C5-H) ppm. $^{13}C\{^1H\}$ NMR ($CDCl_3$): δ = 18.92 (*C*H_3=CN), 20.66 (*C*H_3Ph), 55.08 (*C*H_2*C*H_2), 121.15 (quaternary carbon), 124.73 (aromatic C), 128.22 (aromatic C), 132.93 (aromatic C), 163.79 (quaternary carbon), 170.37 (*C*=N) ppm.

Synthesis of 7,7′dmsalen: This ligand was synthesized starting from hydroxyacetophenone (10.0 g, 73 mmol) and ethylendiamine (2.52 mL, 36.7 mmol) according to the procedure used for 4,4′,7,7′tmsalen.[4] Yield 10.3 g (95%). $C_{18}H_{20}N_2O_2$ (296.36.): calcd. C 72.9, H 6.80, N 9.45; found C 72.9, H 6.88, N 9.47. ES-MS (CH_3OH): *m*/*z* (%) 297.2 (100) [M + H$^+$]. ^1H NMR ($CDCl_3$): δ = 2.38 (s, 6 H, CH_3-C=N), 3.98 (s, 4 H, CH_2-CH_2), 6.79 (m, 2 H, C4-H) 6.92 (m, 2 H, C2-H), 7.28 (m, 2 H, C3-H), 7.53 (m, 2 H, C5-H), 15.90 (s, 2 H, O*H*) ppm. $^{13}C\{^1H\}$ NMR ($CDCl_3$): δ = 14.73 (*C*H_3=CN), 50.16 (*C*H_2*C*H_2), 117.35 (*C*4), 118.44 (*C*2), 119.44 (quaternary carbon), 128.13 (*C*5), 132.43 (*C*3), 163.13 (quaternary carbon), 172.68 (*C*=N) ppm.

Synthesis of [Co(7,7′dmsalen)(py)$_2$]ClO$_4$: This complex was synthesized following the method described previously for [Co(4,4′,7,7′tmsalen)(py)$_2$]ClO$_4$,[4] starting from 7,7′dmsalen (3.0 g, 10.1 mmol) and $Co(OCOCH_3)_2{\cdot}4H_2O$ (2.6 g, 10.4 mmol). Yield 5.8 g (94%). $C_{28}H_{28}ClCoN_4O_2$ (610.93): calcd. C 55.0, H 4.62, N 9.17; found C 54.7, H 4.61, N 9.12. ES-MS (CH_3OH): *m*/*z* (%) 353.1 (100) [M – 2 py]. ^1H NMR ($CDCl_3$): δ = 2.86 (s, 6 H, CH_3-C=N), 4.25 (s, 4 H, CH_2-CH_2), 6.50 (m, 2 H, C4-H), 7.23 (m, 8 H, C3-H, C2-H and *H meta* py), 7.38 (m, 2 H, C5-H), 7.63 (m, 2 H, *H para* py), 8.21 (d, ^3J = 5.3 Hz, 4 H, *H ortho* py) ppm. $^{13}C\{^1H\}$ NMR (67.8 MHz, $CDCl_3$): δ = 20.18 (*C*H_3=CN), 54.20 (*C*H_2*C*H_2), 115.98 (*C*4), 121.05 (quaternary carbon), 124.47 (*C*2), 125.09 (*C* meta py), 130.34 (*C*5), 134.03 (*C*3), 139.01 (*C* para py), 152.70 (*C* ortho py), 165.17 (quaternary carbon), 176.24 (*C*=N) ppm.

Caution: Perchlorate salts of metal complexes with organic ligands are potentially explosive.

Synthesis of [(ClCH$_2$)Co(7,7′dmsalen)]$_2$: This compound was synthesized according to the procedure reported for [(ClCH$_2$)-Co(4,4′,7,7′tmsalen)]$_2$[5] starting from [Co(7,7′dmsalen)(py)$_2$]ClO$_4$ (0.5 g, 0.82 mmol). Yield 246 mg (75%). $C_{38}H_{40}Cl_2Co_2N_4O_4$ (805.52): calcd. C 56.7, H 5.00, N 6.95; found C 55.6, H 5.13, N 6.73. ES-MS (CH_3OH): *m*/*z* (%) 403.0 (28) [M/2 + H], 353.1 (100) [M/2 – ClCH$_2$]. ^1H NMR ([D$_6$]DMSO): δ = 2.47 (s, 6 H, CH_3-C=N), 3.88 (m, 4 H, CH_2-CH_2), 5.13 (s, 2 H, CH_2Cl), 6.40 (m, 2 H, Ph-H), 6.84 (m, 2 H, Ph-H), 7.04 (m, 2 H, Ph-H), 7.49 (m, 2 H, Ph-H) ppm. $^{13}C\{^1H\}$ NMR ([D$_6$]DMSO): δ = 18.96 (*C*H_3=CN), 54.52 (*C*H_2*C*H_2), 113.30 (aromatic carbon), 122.13 (quaternary carbon), 123.54 (aromatic carbon), 130.53 (aromatic carbon), 131.84 (aromatic carbon), 166.47 (quaternary carbon), 169.38 (*C*=N) ppm.

Synthesis of [{(ClCH$_2$)Co(7,7′dmsalen)}$_2$CoCl$_2$] (3): A solution of $CoCl_2{\cdot}6H_2O$ (0.0148 g, 0.062 mmol) in acetone (2 mL) was added to a suspension of [(ClCH$_2$)Co(7,7′dmsalen)]$_2$ (0.050 g, 0.062 mmol) in CH_2Cl_2 (8 mL). The beaker was left overnight covered with Parafilm®. The resulting solution was filtered and set aside in the hood for crystallization. Partial evaporation of the solvent produced a dark solid, which was collected by filtration and kept over P_2O_5 overnight. X-ray quality crystals were obtained by slow evaporation of the reaction mixture. Yield 48 mg (74%). UV/Vis (CH_2Cl_2): λ_{max} (ε) = 245 (9.73×10^4), 323 (2.19×10^4), 524 nm (1.68×10^3 M^{-1}cm^{-1}).

Preparation of [{RCo(4,4′,7,7′tmsalen)}$_2$CoCl$_2$] (R = CH$_3$, CD$_3$) in situ: [RCo(4,4′,7,7′tmsalen)]$_2$ (8.8×10^{-3} mmol) was dissolved in 0.6 mL of $CDCl_3$ in an NMR tube and 8.8 μL of a 1.0 M solution of $CoCl_2{\cdot}6H_2O$ in CD_3OD (8.8×10^{-3} mmol) was added.

^{1}H NMR Titration: [(ClCH$_2$)Co(4,4′,7,7′tmsalen)]$_2$ (14 mg, 1.6×10^{-2} mmol) was dissolved in $CDCl_3$ (0.6 mL) and successive aliquots of a 1 M solution of $CoCl_2$ in 2-propanol were added up to the stoichiometric amount (1:1).

UV/Vis Titration: 3 mL of a stock solution of [(ClCH$_2$)Co-(4,4′,7,7′tmsalen)]$_2$ (5.2 mg, 0.6×10^{-2} mmol) in CH_2Cl_2/2-propanol (100 mL) was titrated with a 0.01 M solution of $CoCl_2$ in 2-propanol up to a 1:8 molar ratio using a Gilson micropipette. The spectra were recorded in the range 300–500 nm.

Table 7. Crystallographic data and details of structure refinements for compounds **1**–**3**.

	1·0.25(CH_2Cl_2)	**2**	**3**·0.75($CHCl_3$)
Formula	$C_{42.25}H_{48.50}Cl_{4.50}Co_3N_4O_4$	$C_{48}H_{52}Cl_{14}Co_3F_6N_4O_4$	$C_{38.75}H_{41.50}Cl_{5.50}Co_3N_4O_4$
M_r	1012.67	1536.03	999.02
Crystal system	orthorhombic	monoclinic	monoclinic
Space group	$Pna2_1$	$P2_1/c$	$P2_1/n$
a [Å]	48.322(18)	14.329(3)	14.868(4)
b [Å]	11.588(3)	13.754(3)	11.079(4)
c [Å]	17.357(4)	16.363(4)	29.458(5)
β [°]		99.38(3)	95.56(3)
Volume [Å^3]	9719(5)	3181.7(12)	4830(2)
Z	8	2	4
$D_{calcd.}$ [g cm^{-3}]	1.384	1.603	1.374
μ Mo-K_α [mm^{-1}]	1.301	1.422	1.362
F(000)	4156	1546	2034
θ_{max} [°]	25.14	23.26	25.68
Unique reflections	8955	4490	9141
Observed reflections [$I > 2\sigma(I)$]	6355	2956	5674
Parameters	1040	386	522
Goodness of fit (F^2)	0.986	1.021	0.956
*R*1 [$I > 2\sigma(I)$][a]	0.0524	0.0570	0.0786
*wR*2[a]	0.1315	0.1591	0.2354
Flack parameter	0.088(19)	–	–
$\Delta\rho$ [e/Å^3]	0.993, –0.337	0.773, –0.644	1.416, –0.537

[a] $R1 = \Sigma||F_o| - |F_c||/\Sigma|F_o|$, $wR2 = [\Sigma w(F_o^2 - F_c^2)^2/\Sigma w(F_o^2)^2]^{1/2}$.

X-ray Crystallography: Crystal data and details of data collection and refinement for the structures reported are summarized in Table 7. Intensity data were collected on a Nonius DIP-1030H system (Mo-K_α radiation, λ = 0.71073 Å) at room temperature for **1** and **2**, and at 200 K for **3**. Cell refinement, indexing, and scaling of the data sets were performed with the programs Denzo and Scalepack.[18] All the structures were solved by direct methods and subsequent Fourier analyses[19] and refined by the full-matrix least-squares method based on F^2 with all observed reflections.[19] Fourier difference maps for **1** and **3** revealed disordered molecules of CH_2Cl_2 accounting for 0.25 and 0.75 molecules per complex unit. H atoms were included at calculated positions in the final cycles of refinement. All calculations were performed using the WinGX System, vers. 1.70.00.[20]

CCDC-717829 (for **1**), -717830 (for **2**), and -717831 (for **3**) contain the supplementary crystallographic data for this paper. These data can be obtained free of charge from The Cambridge Crystallographic Data Centre via www.ccdc.cam.ac.uk/data_request/cif.

Supporting Information (see also the footnote on the first page of this article): ORTEP drawings of molecule B of **1** and of complex **3**; spectrophotometric titration of **1** with $CoCl_2$; ^{1}H NMR spectra of **2** and **3**; expansion of the δ = 28–40 ppm region of the ^{1}H NMR spectra of $[\{(ClCH_2)Co(4,4',7,7'tmsalen)\}_2CoCl_2]$, $[\{(CH_3)Co(4,4',7,7'tmsalen)\}_2CoCl_2]$ and $[\{(CD_3)Co(4,4',7,7'tmsalen)\}_2CoCl_2]$; EXSY spectrum of **1**; plots of the chemical shift vs. $1/T$ for complex **1**; dependence of $\ln K$ on $1/T$ for **1** and **2**.

Acknowledgments

Financial support from the Italian Ministero dell'Istruzione, dell'Università e della Ricerca (MIUR), PRIN 2006, is gratefully acknowledged. We thank Dr. Fabio Hollan for recording the mass spectra.

[1] a) N. Bresciani Pahor, M. Forcolin, L. G. Marzilli, L. Randaccio, M. F. Summers, P. J. Toscano, *Coord. Chem. Rev.* **1985**, *63*, 1; b) L. Randaccio, *Comments Inorg. Chem.* **1999**, *21*, 327.
[2] a) D. H. Busch, N. W. Alcock, *Chem. Rev.* **1994**, *94*, 585; b) E. C. Niederhoffer, J. H. Timmons, A. E. Martell, *Chem. Rev.* **1984**, *84*, 137.
[3] a) R. A. Sheldon, J. K. Kochi, *Metal Catalyzed Oxidations of Organic Compounds*, Academic Press, New York, **1981**, p. 215; b) *Oxidase and Related Redox Systems* (Eds.: T. E. King, H. S. Mason, M. Morrison), University Park Press, Baltimore, **1973**, vol. 1 and 2; c) N. S. Venkataramanan, G. Kuppuraj, S. Rajagopal, *Coord. Chem. Rev.* **2005**, *249*, 1249; d) C. L. Bailey, R. S. Drago, *Coord. Chem. Rev.* **1987**, *79*, 321.
[4] R. Dreos, G. Nardin, L. Randaccio, P. Siega, G. Tauzher, V. Vrdoljak, *Inorg. Chim. Acta* **2003**, *349*, 239.
[5] R. Dreos, G. Nardin, L. Randaccio, P. Siega, G. Tauzher, V. Vrdoljak, *Inorg. Chem.* **2003**, *42*, 6805.
[6] R. Dreos, P. Siega, *Organometallics* **2006**, *25*, 5180.
[7] a) E. Sinn, C. M. Harris, *Coord. Chem. Rev.* **1969**, *4*, 391; b) N. Bresciani-Pahor, M. Calligaris, P. Delise, G. Nardin, L. Randaccio, E. Zotti, G. Facchinetti, C. Floriani, *J. Chem. Soc., Dalton Trans.* **1976**, 2310; c) C. Floriani, F. Calderazzo, L. Randaccio, *J. Chem. Soc., Chem. Commun.* **1973**, 384.
[8] *Biomimetic Oxidations Catalyzed by Transition Metals* (Ed.: B. Meunier), Imperial College Press, London, **2000**.
[9] S. J. Lippard, J. M. Berg, *Principles of Bioinorganic Chemistry*, University Science Books, Mill Valley, CA, **1994**.
[10] a) C. Fukuhara, E. Asato, T. Shimoji, K. Katsura, M. Mori, K. Matsumoto, S. Ooi, *J. Chem. Soc., Dalton Trans.* **1987**, 1305; b) S. Chattopadhyay, G. Bocelli, A. Musatti, A. Ghosh, *Inorg. Chem. Commun.* **2006**, *9*, 1053; c) X. He, C.-Z. Lu, C.-D. Wu, *J. Coord. Chem.* **2006**, *59*, 977; d) S. Banerjee, J.-T. Chen, C.-Z. Lu, *Polyhedron* **2007**, *26*, 686; e) S. Chattopadhyay, M. G. B. Drew, A. Ghosh, *Eur. J. Inorg. Chem.* **2008**, 1693; f) J. Welby, L. N. Rusere, J. M. Tanski, L. A. Tyler, *Inorg. Chim. Acta* **2009**, *362*, 1405; g) A. Ray, G. M. Rosair, R. S. Kadam, *Polyhedron* **2009**, *28*, 796.
[11] *NMR of Paramagnetic Molecules*: *Principles and Applications* (Eds.: G. N. La Mar, W. D. Horrocks Jr., R. H. Holm), Academic Press, New York, **1973**, p. 249.
[12] The complexes of the series (4,4',7,7'tmsalen) are dimers or pentacoordinate in the solid state and hexacoordinate (solvated) or pentacoordinate in solution (see ref. [4]).
[13] M. Calligaris, G. Nardin, L. Randaccio, *Coord. Chem. Rev.* **1977**, *385*, 403.
[14] a) A. Gerli, K. S. Hagen, L. G. Marzilli, *Inorg. Chem.* **1991**, *30*, 4613; b) D.-H. Shi, Z.-L. You, C. Xu, Q. Zhang, H.-L. Zhu, *Inorg. Chem. Commun.* **2007**, *10*, 404; c) Z.-L. You, H.-L. Zhu, W.-S. Liu, *Acta Crystallogr., Sect. E* **2004**, *60*, m1900; d) Y.-P. Diao, S.-S. Huang, H.-L. Zhang, S. Deng, K.-X. Liu, *Acta Crystallogr., Sect. E* **2007**, *63*, m1694.
[15] I. Bertini, C. Luchinat, *Coord. Chem. Rev.* **1996**, *150*, 1.
[16] a) A. Dei, *Inorg. Chem.* **1979**, *18*, 891; b) L. J. Ming, H. G. Jang, L. Que Jr., *Inorg. Chem.* **1992**, *31*, 359; c) J. D. Epperson, L.-J. Ming, B. D. Woosley, G. R. Baker, G. R. Newkome, *Inorg. Chem.* **1999**, *38*, 4498.
[17] a) D. F. Evans, *J. Chem. Soc.* **1959**, 2003; b) D. H. Live, S. I. Chan, *Anal. Chem.* **1970**, *42*, 791; c) D. Ostfeld, I. A. Cohen, *J. Chem. Educ.* **1972**, *49*, 829; d) E. M. Schubert, *J. Chem. Educ.* **1992**, *69*, 62.
[18] Z. Otwinowski, W. Minor, *Processing of X-ray Diffraction Data Collected in Oscillation Mode*, in *Methods in Enzymology*, vol. 276: *Macromolecular Crystallography*, part A, pp. 307–326, **1997** (Eds.: C. W. Carter Jr., R. M. Sweet), Academic Press.
[19] G. M. Sheldrick, *SHELX97 Programs for Crystal Structure Analysis* (rel. 97-2), University of Göttingen, Germany, **1998**.
[20] L. J. Farrugia, *J. Appl. Crystallogr.* **1999**, *32*, 837.

Received: February 4, 2009
Published Online: May 7, 2009

